Region-specific alterations in brain development in one- to three-year-old boys with fragile X syndrome

Fumiko Hoeft[a,1], John C. Carter[a,1], Amy A. Lightbody[a], Heather Cody Hazlett[b], Joseph Piven[b], and Allan L. Reiss[a,2]

[a]Center for Interdisciplinary Brain Sciences Research, Stanford University School of Medicine, Stanford, CA 94305-5795; and [b]The Carolina Institute for Developmental Disabilities, CB# 3366, University of North Carolina, Chapel Hill, NC 27514

Edited by Bruce S. McEwen, The Rockefeller University, New York, NY, and approved April 13, 2010 (received for review March 4, 2010)

Longitudinal neuroimaging investigation of fragile X syndrome (FXS), the most common cause of inherited intellectual disability and autism, provides an opportunity to study the influence of a specific genetic factor on neurodevelopment in the living human brain. We examined voxel-wise gray and white matter volumes (GMV, WMV) over a 2-year period in 1- to 3-year-old boys with FXS (n = 41) and compared these findings to age- and developmentally matched controls (n = 28). We found enlarged GMV in the caudate, thalamus, and fusiform gyri and reduced GMV in the cerebellar vermis in FXS at both timepoints, suggesting early, possibly prenatal, genetically mediated alterations in neurodevelopment. In contrast, regions in which initial GMV was similar, followed by an altered growth trajectory leading to increased size in FXS, such as the orbital gyri, basal forebrain, and thalamus, suggests delayed or otherwise disrupted synaptic pruning occurring postnatally. WMV of striatal-prefrontal regions was greater in FXS compared with controls, and group differences became more exaggerated over time, indicating the possibility that such WM abnormalities are the result of primary FMRP-deficiency-related axonal pathology, as opposed to secondary connectional dysregulation between morphologically atypical brain structures. Our results indicate that structural abnormalities of different brain regions in FXS evolve differently over time reflecting time-dependent effects of FMRP deficiency and provide insight into their neuropathologic underpinnings. The creation of an early and accurate human brain phenotype for FXS in humans will significantly improve our capability to detect whether new disease-specific treatments can "rescue" the FXS phenotype in affected individuals.

early childhood | longitudinal | MRI | voxel-based morphometry

Fragile X syndrome (FXS) is the most common cause of inherited intellectual disability. The condition is caused by expansion of the CGG repeat in the 5′-untranslated region of the fragile X mental retardation 1 (*FMR1*) gene, resulting in hypermethylation, transcriptional silencing, and reduction or loss of the gene product, the fragile X mental retardation protein (FMRP) (1). Loss of FMRP disrupts dendritic maturation, synaptic plasticity, and cerebral development (2). Although much is understood about the typical pattern of cerebral abnormality in adults and older children with FXS, relatively little is known about the evolving nature of these abnormalities in early childhood. One of the most consistent observations in FXS is enlargement of the caudate nucleus, which has been noted in children as young as 18 months (3), relative to both typically developing children and those with idiopathic developmental delay (4). Increased caudate size also shows a negative correlation with FMRP, indicating a genetic dose–response relationship (4, 5). Another consistent finding is reduced size of the cerebellar vermis, which has been observed in FXS across a wide range of ages (4–7). Vermis size has been shown to be positively correlated with FMRP (5), although in our recent study with a more restricted and young age range (ages 1 to 3), this correlation was not observed (4).

Such observations suggest that the *FMR1* mutation and consequent reductions in FMRP levels differentially affect the development of several brain structures. Synapse development, including maturation and pruning, occurs in waves throughout the brain, both pre- and postnatally, and brain regions may undergo this process at different rates (8). Deficient FMRP results in synaptic abnormalities, namely long, thin dendritic spines characteristic of early development (9, 10). Further, recent research in the mouse model of FXS suggests that FMRP plays a critical role during specific periods of cortical development, particularly for regions related to sensory processing (11). The results of this study emphasize the importance of defining critical windows of brain development during which targeted therapy might be most effective.

Taken together, findings to date indicate that certain brain regions are differentially sensitive to the impact of FMRP relative to others, and the maturational period(s) during which FMRP plays a critical role in brain development may differ from region to region. Increasingly divergent trajectories of neurodevelopment leading to regional enlargement after birth, for example, may represent a lack of synaptic pruning and maturation postnatally, whereas persistent regional diminution present from birth might be related to earlier, prenatal effects resulting from deficient FMRP. Thus, it could be hypothesized that regional differences in brain volumes in FXS could serve as temporal markers of FMRP's impact on neurodevelopment.

To address these questions, we examined longitudinal changes in regional gray and white matter volumes (GMV and WMV, respectively) by using modulated voxel-based morphometry (VBM) and Diffeomorphic Anatomical Registration Through Exponentiated Lie Algebra (DARTEL). Participants were 1- to 3-year-old boys [mean = 2.79, SD = 0.63) with FXS (n = 41) or matched-controls [typically developing (TD): n = 21; idiopathic developmental delay (DD): n = 7] who were followed up for an average of 2.03 years (SD = 0.37) (Table 1; regional brain volumes for TD and DD reported separately in Table S1).

Results

Whole-brain voxel-wise analysis showed a main effect of time with GMV increasing over time in most regions (Fig. 1*A*). No region showed significant decrease in GMV over time. There was a main effect of diagnosis with FXS showing significantly greater GMV compared with TD/DD controls in bilateral caudate and also in the nucleus accumbens, putamen, thalamus, hypothalamus, dorsomedial, dorsolateral and ventrolateral prefrontal cortices, and parieto-temporal and occipito-temporal regions, including fusiform gyri, and culmen and declive of the cerebel-

Author contributions: A.A.L., H.C.H., J.P., and A.L.R. designed research; A.A.L., H.C.H., J.P., and A.L.R. performed research; J.P. and A.L.R. contributed new reagents/analytic tools; F. H., J.C.C., A.A.L., H.C.H., J.P., and A.L.R. analyzed data; and F.H., J.C.C., and A.L.R. wrote the paper.

The authors declare no conflict of interest.

This article is a PNAS Direct Submission.

Freely available online through the PNAS open access option.

[1]F.H. and J.C.C. contributed equally to this work.

[2]To whom correspondence should be addressed. E-mail: reiss@stanford.edu.

This article contains supporting information online at www.pnas.org/lookup/suppl/doi:10.1073/pnas.1002762107/-/DCSupplemental.

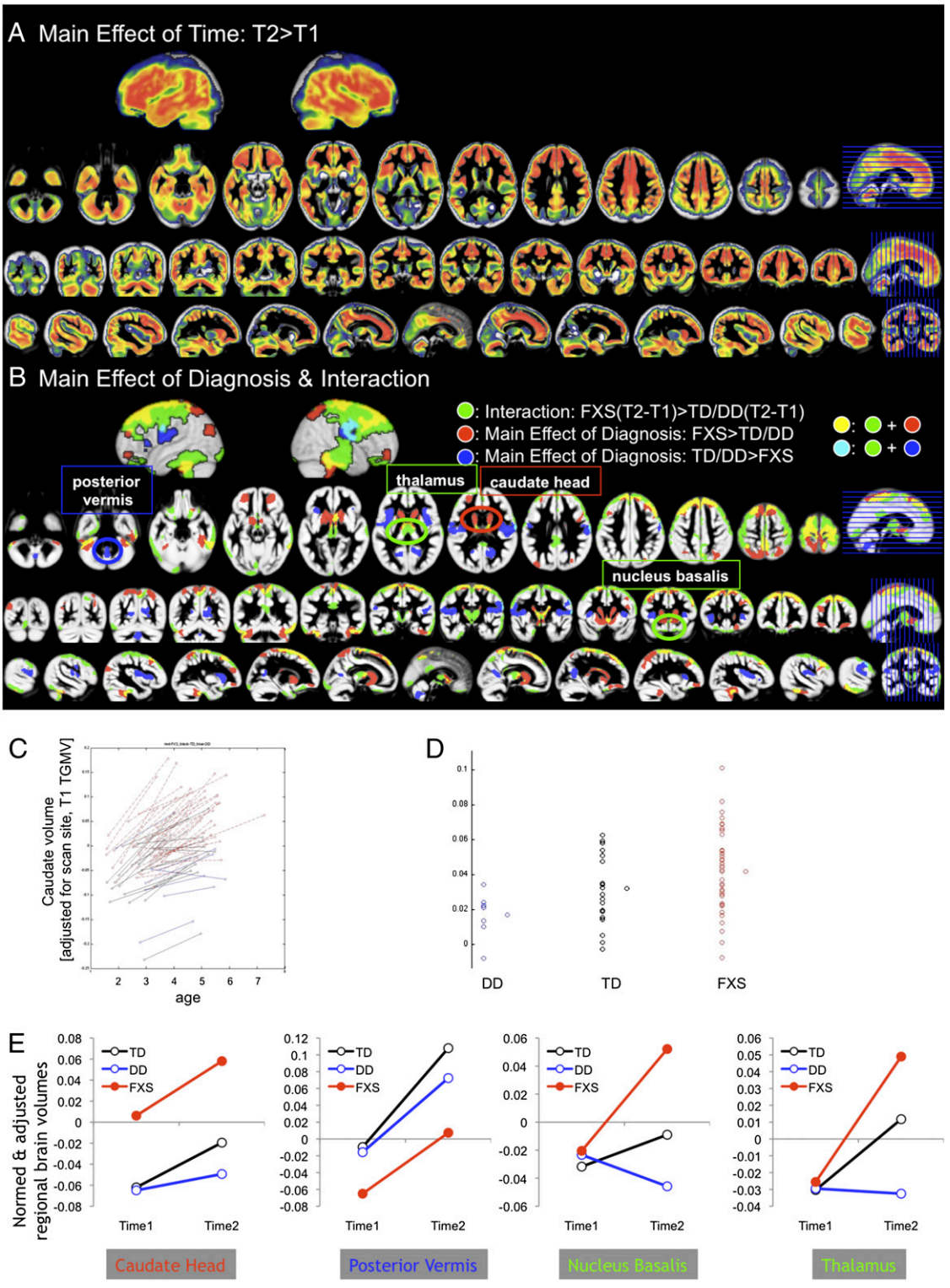

Fig. 1. Differences in regional gray matter volume between groups and over time. (*A*) Regions that show a significant main effect of time. (*B*) Regions that show a significant main effect of diagnosis (red and blue) and a significant interaction effect (green). (*C*) As an example, regional volume of the caudate body that showed an interaction effect is extracted and plotted for each group. (*D*) Same data but slope of caudate volume is plotted for each group. (*E*) Regions highlighted in *B* are plotted as examples of main effect of diagnosis (FXS > TD/DD, caudate head, TD/DD > FXS, posterior vermis) and interaction effects (nucleus basalis, thalamus). Note that the nucleus basalis, cerebellum, and hippocampus are regions with enhanced *FMR1* expression during development. DD, blue; TD, black; FXS, red. Time1 age, total GMV, and scan-site are entered as nuisance variables. $P = 0.05$ corrected.

lum (Fig. 1*B*, red and yellow; peaks reported in Table S2). In the opposite direction, FXS showed reduced GMV compared with TD/DD controls strongly in bilateral insula but also in precuneus/posterior cingulate and posterior cerebellar vermis (Fig. 1*B*, blue and cyan; peaks reported in Table S2). There was also an interaction effect where FXS showed significantly greater

increase in GMV over time compared with TD/DD controls in the following regions: bilateral thalamus, hypothalamus, a small portion of the caudate body, nucleus basalis, amygdala, nucleus accumbens, dorsomedial (superior frontal and medial frontal gyri), dorsolateral (middle frontal gyrus), ventromedial (rectal and orbital gyri) and ventrolateral prefrontal cortices (inferior frontal gyrus), temporal (superior, middle, and inferior temporal gyri) and occipital regions, including fusiform gyri, and culmen and declive of the cerebellum (Fig. 1*B*, green, yellow, and cyan; peaks reported in Table S2). There were no other significant interaction effects.

In the white matter (WM), there was also a main effect of time with WM increasing over time in most WM regions (Fig. 2*A*). No regions showed significant decrease in WMV over time. There was a main effect of diagnosis with FXS showing greater WMV compared with TD/DD controls in bilateral frontostriatal and medial temporal regions (Fig. 2*B*, red and yellow; peaks reported in Table S2). In the opposite direction, FXS showed reduced WMV compared with TD/DD controls in lateral central regions (Fig. 2*B*, blue and cyan; peaks reported in Table S2). There was also an interaction effect where FXS showed a significantly greater increase in WMV over time compared with TD/DD controls. These regions included bilateral dorsal and ventral frontal and fronto-striatal regions and posterior temporal and temporal pole regions (Fig. 2*B*, green, yellow, and cyan; peaks reported in Table S2). There were no other types of interaction effects.

Discussion

In this study, we examined brain MRIs from a longitudinal cohort of young boys with FXS and age- and developmentally matched controls to characterize changes in regional brain volumes over time. Our findings of larger GMV in the caudate and fusiform gyri replicate prior studies of older individuals with FXS (5, 12–14), indicating that these adult-like abnormalities are present from an early age (1-3 years). In these regions, which in our study were larger in FXS at both timepoints, an early, possibly prenatal, alteration of neurodevelopment is likely. On the other hand, regions in which the rate of GMV change was greater in FXS than in controls, such as the orbital gyri, basal forebrain, and large segments of the thalamus, may suggest delayed or otherwise disrupted synaptic pruning occurring postnatally, because GMVs in these areas were initially similar in FXS and controls but became relatively larger in FXS by 3–5 years of age (second timepoint).

WMV changes were noted mainly in tracts running through prefrontal, temporal, and central regions. Differences in these regions may indicate abnormal connectivity as a result of abnormalities in the connected regions themselves or may represent a primary defect of white matter development. Although in the present study these regions were not characterized by tractography, they do share a positional similarity to tracts that have been reported to be abnormal in FXS, including ventral frontostriatal pathways, which show reduced fractional anisotropy and fiber density, the latter of which is associated with lower intelligence quotient in these individuals (15). As WMV in ventral prefrontal tracts increased over time at a greater rate in FXS, and because FMRP is thought to regulate axonal development (16) and possibly myelination (17), it is conceivable that white matter abnormalities in ventral frontostriatal tracts in FXS are the result of primary FMRP-deficiency-related axonal pathology, as opposed to secondary connectional dysregulation between morphologically atypical brain structures.

It is noteworthy that several regions, which showed differential rates of volume change over time, are known to be rich in FMRP expression, namely the cerebellum, hippocampus, and basal forebrain (nucleus basalis) (18). Curiously, these regions did not show similar rates of volume change over time. It is therefore possible that the neuroanatomic profile in FXS depends not only on the level of FMRP expression in a given brain structure, but

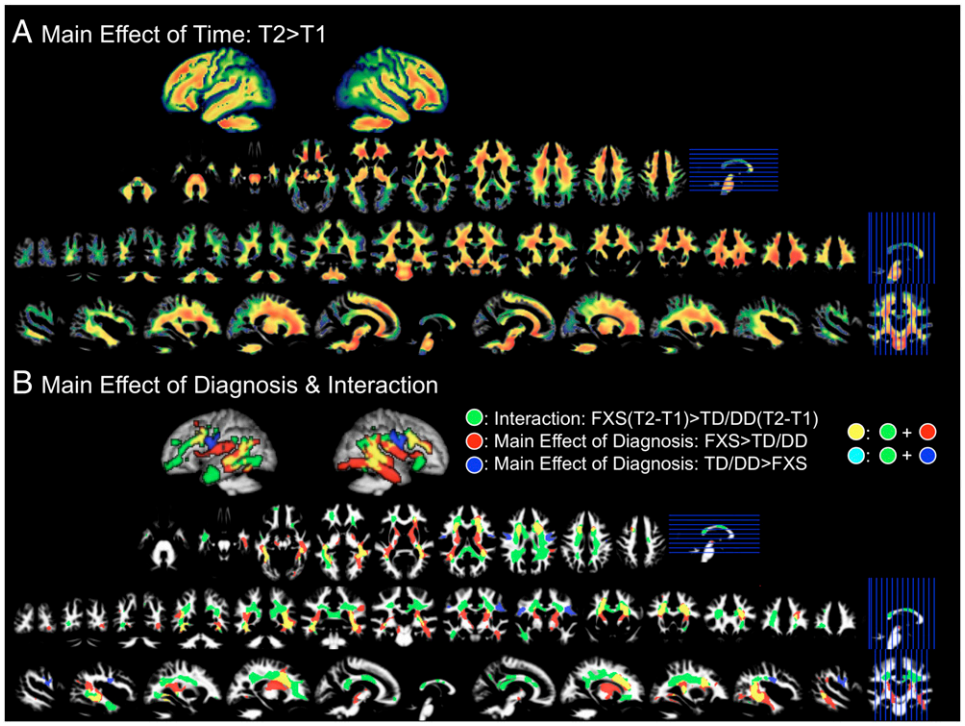

Fig. 2. Differences in regional WMV between groups and over time. (*A*) Regions that show a significant main effect of time. (*B*) Regions that show a significant main effect of diagnosis (red and blue) and a significant interaction effect (green). Time1 age, total WMV, and scan-site are entered as nuisance variables. $P = 0.05$ corrected.

also the differential effects of FMRP on synaptogenesis, dendritic outgrowth, and pruning at various points during the neurodevelopmental process. For example, GMV in the cerebellar vermis was found to be consistently smaller in FXS at both timepoints but changing over time at similar rates to controls. This result suggests that FMRP plays a critical role in this region during a relatively early period, before age 1–3 years and possibly during prenatal neurodevelopment. In the basal forebrain, another region rich in FMRP (18), volumetric differences in gray matter are not seen until later in childhood, indicating that FMRP's critical period of activity in this region is postnatal, likely occurring within the 3- to 5-year range.

In addition to further characterizing the neuroanatomic profile of FXS by extending observations to include longitudinal assessments of very young children, our study provides a basis upon which interventions aimed at curtailing abnormal neurodevelopment can be assessed. Taken together, our results suggest that the neuroanatomic abnormalities of FXS are not laid out simultaneously but rather occur at different times in different regions, consistent with patterns of cortical development (8) and site-specific activity of FMRP (9, 19–21), likely representing a combination of pre- and postnatal processes. As such, it may be possible to track the efficacy of interventional strategies, such as metabotropic glutamate receptor antagonists (22), over time and in specific brain structures, with an understanding of the expected neurodevelopmental course in those structures.

Although our study provides exciting preliminary evidence into the developmental changes of neuroanatomical profiles in FXS, there are important issues that could be addressed in future studies. First, future studies should include larger samples of controls, in particular of individuals with idiopathic DD so that TD and DD controls could be examined separately. Second, tracking development from a younger age and at multiple timepoints for a longer period is desirable. Third, it may be of interest to compare FXS with another population that has genetic abnormalities that affect brain development and some overlap in cognitive abnormalities such as Williams syndrome. Fourth, we did not use manual or atlas-based anatomical parcellation methods to characterize between-group differences in brain development. Utilization of such methods could provide interesting complementary data in a subsequent study of brain development in FXS. However, use of manual or atlas-based methods would be unlikely to converge on the same results as those shown here, because the cortical and subcortical regions showing significant between-group differences with VBM do not correspond to traditional anatomical boundaries.

These data provide the beginnings of brain region-specific developmental trajectories in FXS, reflecting time-dependent effects of FMRP deficiency. Our results indicate that some adult-like patterns of structural abnormalities are present in very young children with FXS, whereas other abnormalities evolve over time differently. It is also notable that our finding of aberrant neurodevelopmental trajectories in the thalamus and cortex of young boys with FXS (Fig. 1*B*) is consistent with the recent report of FMRP effects on excitatory thalamocortical synapses in the somatosensory cortex of the FXS animal model (11). Such data provide insight into the neuropathologic effects of reduced FMRP in early development and underscores the need for longitudinal examination of brain morphology in this population. Lastly, this basic neuroanatomic developmental profile may aid in targeting and evaluating therapeutic modalities that could rescue the FXS phenotype in affected individuals.

Materials and Methods

Participants and Cognitive Assessment. Participants for this study were recruited by Stanford University School of Medicine (SU) and the University of North Carolina-Chapel Hill (UNC). The study protocols were approved by the human subjects committees at SU and UNC, and consent was obtained. TD and DD children were recruited through local intervention programs, preschools, childcare facilities, community media, and state-run agencies (e.g., Regional Center system in California and Child Development Service Agencies in North Carolina). Children with FXS were recruited through registry databases maintained by Stanford and UNC, postings to the National Fragile X Foundation website and quarterly newsletter, and mailings to other regional fragile X organizations. Participants were excluded from the study if they were born preterm (<34 weeks), had a low birth weight (<2,000 grams), showed evidence of a genetic condition or syndrome, exhibited sensory impairments or had any serious medial or neurological condition that affected growth or development (e.g., seizure disorder, diabetes, congenital heart disease). Children in the DD group comprised developmental delays of unknown etiology (with a composite standard score <85 on the Mullen Scales of Early Learning) did not exhibit symptoms indicating an autism spectrum disorder or any symptoms indicative of another developmental disorder (e.g., Down syndrome, Williams syndrome). TD and DD children were screened for autism spectrum disorders by using the Childhood Autism Rating Scale (CARS). All children in these groups scored below the cutoff for the nonautistic range (<30). Details regarding demographic information and distribution of sample between recruitment sites can be found in Table 1. All participants were given a standard battery of cognitive, adaptive, and behavioral measures that included the Mullen Scales of Early Learning (23). There were no significant differences between sites in any of the cognitive measurements for each diagnostic group or when all groups were combined (all $P > 0.05$).

Genotype. All children in the FXS and DD groups underwent DNA testing for the typical FMR1 expansion mutation. This testing confirmed the presence of the mutation in children in the FXS group and ruled out FXS as a cause of delay in the DD groups. To assess the presence of the fragile X mutation, standard Southern blot analysis was performed, followed by FMR1-specific probe hybridization (24). To quantify FMRP expression, the percentage of peripheral lymphocytes containing FMRP was calculated by using immunostaining techniques (25).

MRI Scanning Procedures. Imaging data were acquired between April 2000 and May 2008 at SU (Lucile Packard Children's Hospital) and UNC (Brain Imaging and Analysis Center) by using identical pulse sequences and scanners (General Electric 1.5-T Signa scanner; GE Imaging Systems) at both sites. The pulse sequences used were designed to maximize contrast among GM, WM, and cerebrospinal fluid for the participants' age range. Images acquired included a coronal T1-weighted sequence (inversion recovery preparation pulse = 300 ms; repetition time = 12 ms; echo time = 5 ms; flip angle = 20°; slice thickness = 1.5 mm; number of excitations = 1; field of view = 20 cm; matrix = 256 × 192). A MR quality control phantom was scanned after each participant at both sites to standardize assessment over sites, individuals, and time. Children in the FXS and DD groups were sedated during the MRI. Sedation was administered by a pediatric anesthesiologist, and children were monitored continually during the MRI procedure. TD children were scanned while sleeping, at a time that was later than the participant's normal bedtime. In addition, for the sleep scans, parents were asked to wake their child up slightly earlier on the morning of the scan, and to shorten nap time that day, to increase the likelihood of the child sleeping through the entire scan. To prepare for the scan, families received a packet of materials, including a compact disc of scanner noises designed to sensitize him/her to the scanner sounds. TD children also participated in a simulated MRI session at the laboratory in which they were asked to practice holding still and to mitigate fear should the child awaken during the MRI.

Cross-Site Analysis. To maximize scan compatibility across sites, identical pulse sequences and scanners were used at the two collection sites. In addition, to characterize scanner quality and signal-to-noise ratio (SNR) during our study, we collected phantom scans after each participant. During the course of the study, 24 random phantom scans (12 per scanner, selected across the entire period of the study by a research assistant blind to scans) were used by the method described in ref. 26. Two SNR measurements were performed and were not significantly different across sites ($P = 0.39$ and $P = 0.22$, respectively). We also assessed whether brain volumes within each group differed as a function of scan site. No tissue type [GMV, WMV, or total tissue volume (TTV)] was significantly different across sites (all $P > 0.05$). Finally, we included scan site as a nuisance variable in all reported analyses to mitigate small (nonsignificant) differences found between sites. For more details, see ref. 4.

VBM Processing. VBM analyses of MR images were carried out by using the SPM5 statistical package (http://www.fil.ion.ucl.ac.uk/spm), including the DARTEL toolbox (27) and VBM5.1 (http://dbm.neuro.uni-jena.de/vbm). Images

were bias-field corrected and segmented to GM, WM, and CSF by using VBM 5.1 and custom priors created from all scans. The images were normalized by using the DARTEL toolbox and then to MNI space following the DARTEL guide, which resulted in modulated GM and WM images. Smoothing was performed with an isotropic Gaussian kernel with full-width at half-maximum of 8 mm. For each participant, segmentation and normalization accuracy were manually inspected.

Analyses of Total GM Volume (TGMV), Total WM Volume (TWMV), and Total Tissue Volume (TTV). We examined TGMV, TWMV, and TTV (GMV + WMV) differences between TD, DD, and FXS groups, using values obtained from VBM processing by using analysis of covariance (ANCOVA), covarying out age and site.

Analyses of Regional GMV and WMV. Regional GMV and WMV differences between FXS and controls (TD and DD combined) at time 1 and time 2 were examined by using whole-brain 2 (time) × 2 (group, FXS, and TD + DD) repeated measures ANCOVA, covarying out age, site, duration between times 1 and 2, and TGMV/TWMV for GM and WM analyses, respectively. TD and DD groups were initially grouped together because of the small *n*. Main effect of time, diagnosis, and interaction effects were examined. A statistical threshold of $P = 0.05$ false discovery rate (FDR), extent threshold = 200 voxels, was used (28) and was corrected for nonisotropic smoothness (29, 30). Statistical images were overlaid on the average GM and WM images from all subjects, using MRIcron (www.sph.sc.edu/comd/rorden/mricron/). Talairach coordinates of peaks of significant clusters were converted from MNI space by using the mni2tal function (www.mrc-cbu.cam.ac.uk/Imaging/Common/mnispace.shtml). Talairach Daemon (Research Imaging Center, University of Texas Health Science Center) and the atlas by Talairach and Tournoux (31) were initially used to identify Brodmann Areas. The final anatomic locations are reported according to their anatomic location overlaid on the custom template.

ACKNOWLEDGMENTS. We sincerely thank all of the families who made this study possible. We also thank Chad Chappell, MA; Nancy Garrett, BA; Michael Graves, MChe; Cindy Hagan, BA; Cindy Johnston, MS; Judy Morrow, PhD; Robin Morris, BA; Rachel Smith, BA; Arianna Martin, BA; Cristiana Vattuone, BA; Christa Watson, BA; Anh Weber, PhD; Masanori Nagamine, MD/PhD; Kelly Chen, BS; and Sweta Patnaik, MS who were involved in data collection and/or processing. This study was funded by MH64708-05 (to A.L. R. and J.P.), MH61696 (to J.P.), HD03110-36 (to J.P.), MH050047 (to A.L.R.), and the Canel family fund, and F.H. was funded by National Alliance for Research on Schizophrenia and Depression Young Investigator Award, Stanford Child Health Spectrum, and National Institute of Child Health and Human Development HD054720.

1. Verkerk AJ, et al. (1991) Identification of a gene (FMR-1) containing a CGG repeat coincident with a breakpoint cluster region exhibiting length variation in fragile X syndrome. *Cell* 65:905–914.
2. Greenough WT, et al. (2001) Synaptic regulation of protein synthesis and the fragile X protein. *Proc Natl Acad Sci USA* 98:7101–7106.
3. Hazlett HC, et al. (2009) Teasing apart the heterogeneity of autism: Same behavior, different brains in toddlers with fragile X syndome and autism. *J Neurodev Disord* 1: 81–90.
4. Hoeft F, et al. (2008) Morphometric spatial patterns differentiating boys with fragile X syndrome, typically developing boys, and developmentally delayed boys aged 1 to 3 years. *Arch Gen Psychiatry* 65:1087–1097.
5. Gothelf D, et al. (2008) Neuroanatomy of fragile X syndrome is associated with aberrant behavior and the fragile X mental retardation protein (FMRP). *Ann Neurol* 63:40–51.
6. Mostofsky SH, et al. (1998) Decreased cerebellar posterior vermis size in fragile X syndrome: Correlation with neurocognitive performance. *Neurology* 50:121–130.
7. Reiss AL, Aylward E, Freund LS, Joshi PK, Bryan RN (1991) Neuroanatomy of fragile X syndrome: the posterior fossa. *Ann Neurol* 29:26–32.
8. Huttenlocher PR, Dabholkar AS (1997) Regional differences in synaptogenesis in human cerebral cortex. *J Comp Neurol* 387:167–178.
9. Irwin SA, Galvez R, Greenough WT (2000) Dendritic spine structural anomalies in fragile-X mental retardation syndrome. *Cereb Cortex* 10:1038–1044.
10. Weiler IJ, Greenough WT (1999) Synaptic synthesis of the Fragile X protein: Possible involvement in synapse maturation and elimination. *Am J Med Genet* 83:248–252.
11. Harlow EG, et al. (2010) Critical period plasticity is disrupted in the barrel cortex of FMR1 knockout mice. *Neuron* 65:385–398.
12. Kates WR, Folley BS, Lanham DC, Capone GT, Kaufmann WE (2002) Cerebral growth in Fragile X syndrome: Review and comparison with Down syndrome. *Microsc Res Tech* 57:159–167.
13. Lee AD, et al. (2007) 3D pattern of brain abnormalities in Fragile X syndrome visualized using tensor-based morphometry. *Neuroimage* 34:924–938.
14. Reiss AL, Dant CC (2003) The behavioral neurogenetics of fragile X syndrome: Analyzing gene-brain-behavior relationships in child developmental psychopathologies. *Dev Psychopathol* 15:927–968.
15. Haas BW, et al. (2009) Early white-matter abnormalities of the ventral frontostriatal pathway in fragile X syndrome. *Dev Med Child Neurol* 51:593–599.
16. Hengst U, Cox LJ, Macosko EZ, Jaffrey SR (2006) Functional and selective RNA interference in developing axons and growth cones. *J Neurosci* 26:5727–5732.
17. Wang H, et al. (2004) Developmentally-programmed FMRP expression in oligodendrocytes: A potential role of FMRP in regulating translation in oligodendroglia progenitors. *Hum Mol Genet* 13:79–89.
18. Abitbol M, et al. (1993) Nucleus basalis magnocellularis and hippocampus are the major sites of FMR-1 expression in the human fetal brain. *Nat Genet* 4:147–153.
19. Hanson JE, Madison DV (2007) Presynaptic FMR1 genotype influences the degree of synaptic connectivity in a mosaic mouse model of fragile X syndrome. *J Neurosci* 27: 4014–4018.
20. Galvez R, Greenough WT (2005) Sequence of abnormal dendritic spine development in primary somatosensory cortex of a mouse model of the fragile X mental retardation syndrome. *Am J Med Genet A* 135:155–160.
21. Irwin SA, et al. (2005) Fragile X mental retardation protein levels increase following complex environment exposure in rat brain regions undergoing active synaptogenesis. *Neurobiol Learn Mem* 83:180–187.
22. Yan QJ, Rammal M, Tranfaglia M, Bauchwitz RP (2005) Suppression of two major Fragile X Syndrome mouse model phenotypes by the mGluR5 antagonist MPEP. *Neuropharmacology* 49:1053–1066.
23. Mullen EM (1995) *Mullen Scales of Early Learning AGS Edition* (American Guidance Service, Circle Pines, MN).
24. Oberle I, et al. (1991) Instability of a 550-base pair DNA segment and abnormal methylation in fragile X syndrome. *Science* 252:1097–1102.
25. Willemsen R, et al. (1995) Rapid antibody test for fragile X syndrome. *Lancet* 345: 1147–1148.
26. Henkelman RM (1985) Measurement of signal intensities in the presence of noise in MR images. *Med Phys* 12:232–233.
27. Ashburner J (2007) A fast diffeomorphic image registration algorithm. *Neuroimage* 38:95–113.
28. Genovese CR, Lazar NA, Nichols T (2002) Thresholding of statistical maps in functional neuroimaging using the false discovery rate. *Neuroimage* 15:870–878.
29. Hayasaka S, Phan KL, Liberzon I, Worsley KJ, Nichols TE (2004) Nonstationary cluster-size inference with random field and permutation methods. *Neuroimage* 22:676–687.
30. Worsley KJ, Andermann M, Koulis T, MacDonald D, Evans AC (1999) Detecting changes in nonisotropic images. *Hum Brain Mapp* 8:98–101.
31. Talairach J, Tournoux P (1988) *Co-planar Stereotaxic Atlas of the Human Brain* (Thieme, New York).